

Vertical Protection Level Equations for Dual Frequency SBAS

Todd Walter, Juan Blanch, and Per Enge,
Stanford University

ABSTRACT

The L1-only Satellite-Based Augmentation System (SBAS) Minimum Operational Performance Standards (MOPS) were developed long before any SBASs were certified for operation. During the development and certification of the Wide Area Augmentation System (WAAS), it was discovered that the zero-mean Gaussian basis of the Vertical Protection Level (VPL) equation was not strictly true for some error sources, and very difficult to sufficiently demonstrate for others. The actual data collected in support of system performance demonstrated non-Gaussian behavior. Further, sources of small uncorrectable biases were discovered after the original MOPS development. These biases can arise from consistent, minor differences in the signal structure from one satellite to another. Antenna biases at the satellite, at the reference stations, and at the user are other possible sources of these biases. Because the MOPS VPL equation is based upon zero-mean Gaussian error combination, much additional work was required to demonstrate that the actual errors could be sufficiently protected safely. Some performance is lost because the system has to implement conservative approaches to account for these discrepancies.

The advent of dual frequency SBAS affords the opportunity to revisit the MOPS and use different approaches for this new class of user. Lessons learned from the L1-only system certification and operation can be leveraged to both ease development of the future dual frequency system and improve user performance. This paper examines the VPL equations and proposes changes to directly address these lessons. The handling of non-Gaussian behavior and small biases directly address both goals. The VPL can be further changed to directly address the threats that most limit availability. Without the corrupting influence of the ionosphere, satellite faults become the dominant source of significant error. New VPL equations are proposed to specifically account for individual satellite fault modes. This paper will demonstrate that by avoiding overly conservative steps required to handle all possible cases, the users will see reduced protection levels and higher availability.

INTRODUCTION

The Global Positioning System (GPS) is in the process of adding new civil signals [1] [2] [3]. These new civil signals include a second frequency in a protected Aeronautical Radio Navigation Services (ARNS) band that may be used to guide aircraft. The incorporation of this new signal into Satellite-Based Augmentation Systems (SBAS), such as the Federal Aviation Administration's (FAA) Wide Area Augmentation System (WAAS) [4] [5], allows for greatly expanded service and capabilities. Most importantly, the largest source of uncertainty affecting the accuracy and integrity of the system can be directly observed and eliminated in the aircraft. This allows for better levels of service within the existing coverage region and expansion of coverage beyond where the reference station network can adequately monitor the ionosphere.

The addition of a new frequency also provides an opportunity to broadcast a new set of SBAS corrections that can take a different approach than was used on the legacy L1 correction signal. Thus, lessons learned from implementation of the L1-only SBASs can be applied to the development of the L5 correction signal to support L1/L5 signals. The original integrity approach was based upon a simple notion that the actual error distributions would be close to Gaussian and that as they were convolved together the resulting positioning errors would also be close to Gaussian. Although this notion is correct, the small departures from ideal behavior led to challenges in following this approach precisely. In order to protect against non-Gaussian behavior, new approaches were developed to create safe confidence bounding terms to broadcast to the user [6] [7]. However, these approaches usually impose conservative constraints that restrict availability more than necessary. In addition, some of the analyses are cumbersome and time-consuming. A more direct approach could improve availability and simplify the certification of the system.

Previously, it has been suggested to incorporate small nominal bias terms into the computation of the positioning bound [8] [9]. This paper goes even further,

changing the protection level computation to specifically model the known fault modes. The resulting proposal has similarities to other satellite navigation integrity schemes, borrowing elements from the Ground-Based Augmentation System (GBAS) [10], Advanced Receiver Autonomous Integrity Monitoring (ARAIM) [11] [12] [13], and the Galileo Safety-of-Life (SoL) approach [14].

The paper begins by discussing the relative merits of an L1/L5 solution in the aircraft compared to the existing L1-only method. Next we review the L1-only integrity equation and the benefit of adding nominal biases. We then develop the new protection level approach based upon the expected fault modes. The paper then examines a previous study on the accuracy of the existing L1-only system to develop models for the expected accuracy of the future L1/L5 system. These models are used to compare the improvement offered by the proposed changes relative to a more conventional L1/L5 implementation of the existing scheme. Finally conclusions and recommendations are provided.

THE UTILITY OF L1/L5 IN THE AIRCRAFT

GPS satellites originally only offered one civil signal at the GPS L1 frequency (1575.42 MHz). Fortunately this falls in an ARNS band and may be used for civil aviation. It has already been incorporated into several systems to provide guidance to aircraft [15] [5] [10]. Two additional civil frequencies are starting to be added to the GPS satellites. L2 (1227 MHz) is further along, but is not in an

ARNS band and may not be used for aviation. L5 has only just started to be implemented but is in an ARNS band and may be used for aircraft guidance.

The main advantage of having two signals at two distinct frequencies is that the range error caused by the ionosphere may now be directly estimated and removed. The ionosphere is the largest source of uncertainty for single-frequency GPS-based aircraft navigation. Often, the ionospheric delay is small and smoothly varying. However there can be disturbances that create significant variations over time and/or space. L1-only systems must account for this risk as they assess the potential bounds on position errors.

L1/L5 systems are not vulnerable to this uncertainty and can form smaller bounds around the possible positioning error. Table 1 highlights this advantage. The table also identifies a disadvantage with this approach. The ionosphere-free combination of signals increases the dependency on both the L1 and L5 signal errors. Although the combination eliminates dependence on ionospheric delay error and keeps the same dependence on tropospheric and satellite clock and ephemeris errors, other L1 only errors such as multipath are multiplied by 2.26 and L5 only errors are multiplied by 1.26. Thus, if the same level of multipath exists on L1 and L5 the overall contribution is increased to 2.6 times that of L1-only.

We will show this to be a poor trade most of the time, in that the nominal ionosphere accuracy of the WAAS

	iono error	Clock / ephemeris	Tropo error	L1 error	L5 error	RSS
L1 Only	1	1	1	1	0	1
iono-free	0	1	1	$\frac{f_1^2}{f_1^2 - f_5^2} = 2.26$	$\frac{f_5^2}{f_1^2 - f_5^2} = 1.26$	2.6
Nominal Error	0.2 - 1 m	0.3 - 0.5 m	0.05 - 0.5 m	0.15 - 0.5 m	0.15 - 0.5 m	0.4 - 1.3 m
Max Error	50 m	Unlimited	5 m	0.5 m	0.5 m	1.3 m

Table 1. This table shows the dependencies of the L1-only and L1/L5 approaches on different error sources. Also shown are nominal and extreme expected values of the errors.

ionospheric correction is smaller than the increase in the contribution from the airborne multipath. However, at the extremes, the ionosphere delay error can grow much larger than the multipath error. Therefore, the extreme errors are reduced in this trade. It is these extreme errors that we are most interested in for integrity. By reducing them we can reduce the overall position error bound and improve availability.

It may seem incorrect that by adding a new signal we reduce accuracy, but we are really adding a new signal and removing another one: the L1-only ionospheric correction. Removing dependence on the broadcast ionospheric correction greatly expands the coverage region. It is possible to find other ways to combine the different signals, L1 and L5 with the iono delay estimate that improve accuracy and integrity within the coverage region. However, the need to do so has not yet been demonstrated.

SINGLE-FREQUENCY VPL EQUATION

The L1-only protection level equations were developed based upon early prototyping of the WAAS system. The basic notion was that the error sources were approximately Gaussian and that a Gaussian model would be sufficiently accurate to be able to conservatively describe the positioning errors [16]. Therefore, four error terms were developed to describe satellite clock and ephemeris errors, ionospheric delay errors, tropospheric delay errors, and airborne receiver and multipath errors [17]. The conservative variances of these terms were combined to form a conservative variance for the individual pseudorange error.

$$\sigma_i^2 = \sigma_{\text{fit},i}^2 + \sigma_{\text{UIRE},i}^2 + \sigma_{\text{tropo},i}^2 + \sigma_{\text{air},i}^2 \quad (1)$$

This pseudorange variance is inverted and placed on the diagonal elements of the weighting matrix, \mathbf{W} , and combined with the geometry matrix, \mathbf{G} , to form the covariance of the position estimate [16][17].

$$(\mathbf{G}^T \cdot \mathbf{W} \cdot \mathbf{G})^{-1} \quad (2)$$

The third diagonal element represents the conservative estimate of the error variance in the vertical direction. Since the Vertical Protection Level (VPL) is intended to bound 99.99999% of errors it is set to the equivalent Gaussian tail value of 5.33. Thus, the final VPL for L1-only is given by [17].

$$VPL_{\text{SBAS}} = 5.33 \sqrt{[(\mathbf{G}^T \cdot \mathbf{W} \cdot \mathbf{G})^{-1}]_{3,3}} \quad (3)$$

DUAL-FREQUENCY VPL EQUATIONS

One significant difficulty encountered when developing the safety analysis for WAAS and LAAS was the presence of small biases and non-Gaussian behavior observed in data used to validate the analyses. The integrity equations for these systems are based upon zero-mean Gaussian behavior. The sigmas broadcast for use in these equations were inflated to account for worst-case behavior that in turn led to larger protection levels. However, the underlying mathematical assumptions required exactly Gaussian and zero-mean characteristics. Additional analyses were created to ensure that the protection levels were sufficiently large to cover observed imperfect behavior. However, these new analyses imposed additional constraints on the system and further limited performance [18] [7]. Thus, several previous papers [8] [9] [12] advocated the inclusion of nominal bias terms into the protection level equation to account for non zero means and non-Gaussian behavior.

In addition to nominal bias terms, we propose a further change to the protection level equations. The elimination of the ionospheric threats also removes the only significant threat that could introduce large errors on multiple satellite measurements simultaneously. The remaining large threats are satellite specific and include satellite clock/ephemeris error, satellite code carrier divergence, and signal deformations [19] [20]. There are smaller threats than can affect multiple satellite measurements such as multipath and antenna biases at the ground reference equipment, tropospheric errors, and incorrect Earth orientation parameters affecting the conversion of the ephemeris estimate to the terrestrial frame. The proposed protection level formulation addresses all of these threats.

The variances in (1) have been developed as overbounding variances [21] [18] [7]. Figure 1 provides an example of how some of these variances are determined. The error is typically protected in real time by a monitor within WAAS. There is some noise associated with the ability to observe the error. This is represented by the green nominal error distribution at the top of Figure 1. The monitor will have a set threshold that will be used to declare a fault if the observed error becomes too large. However, this threshold must be set sufficiently large such that the monitor is not declaring a fault too often. Typically, in order to meet aircraft

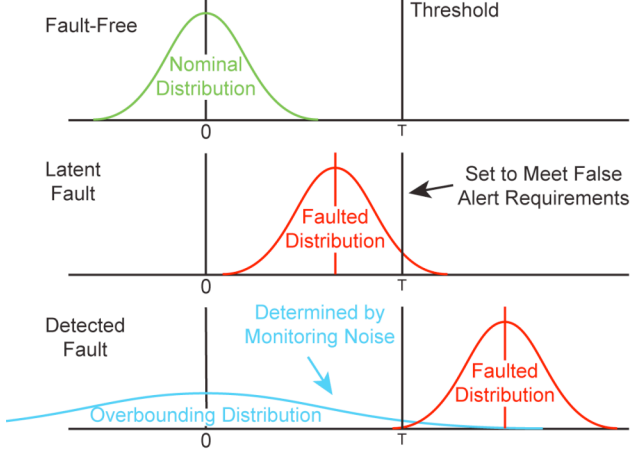


Figure 1. This figure shows the expected nominal fault-free error distribution at the top, with a latent fault in the middle and a detectable fault at the bottom. The measurement error distribution is unchanged by the fault except for the inclusion of the fault bias.

guidance continuity requirements, we would like this monitor to trip less than once a month under nominal conditions.

The middle trace of Figure 1 demonstrates the presence of a small fault that is not yet large enough to assure tripping the monitor. The fault is represented as a bias that does not otherwise affect the uncertainty in observing the error. The bottom part of the figure illustrates the largest error that will only just meet the required probability of missed detection. This probability is represented by the portion of the red curve to the left of the threshold. The magnitude of this largest fault is at the center of this distribution. Because of the observation error, it is larger than the threshold. This largest error must be transmitted to the user so that they properly account for the error. In the single frequency VPL (3) the only way to represent this error is through the broadcast variance. Therefore the sigma value must be at least equal to this largest possible fault divided by 5.33, as represented by the blue distribution at the bottom of Figure 1. Typically this distribution is at least three times larger than the nominal distribution.

Each of the variances in (1) must be inflated in this manner. Thus, the final VPL consists of many simultaneously inflated variances. However, there is no expectation that each error source on each satellite harbors a maximum undetected fault mode. Instead, we know from long observation of system performance that such faults are rarely present on any measurements and never on more than one simultaneously. We propose modifying the VPL equation to exploit this fact. We

recommend the addition of a faulted bias term to the VPL equation and a change in the variance terms to represent the nominal monitoring error rather than an artificially inflated variance to cover the latent fault.

Our proposed equation covers two hypotheses, a nominal fault-free situation, and a separate faulted condition. This approach is similar to that taken by the Ground-Based Augmentation System (GBAS) [22] and recently proposed Advanced Receiver Autonomous Integrity Monitoring (ARAIM) equations [12] [13]. The unfaulted term takes the form of

$$VPL_0 = K_{v,PA} \sqrt{\sum_{i=1}^N S_{3,i}^2 \sigma_{ff,i}^2} + \sum_{i=1}^N |S_{3,i} b_i| \quad (4)$$

where $K_{v,PA}$ corresponds to the Gaussian tail and is expected to be 5.33, $S_{3,i}$ is the third element of the i^{th} row of the projection matrix given by

$$\mathbf{S} = (\mathbf{G}^T \cdot \mathbf{W} \cdot \mathbf{G})^{-1} \cdot \mathbf{G}^T \cdot \mathbf{W} \quad (5)$$

$S_{3,i}$ represents the effect on the vertical position error due to an error on the ranging measurement to the i^{th} satellite. $\sigma_{ff,i}^2$ is the fault-free or nominal error variance and b_i is the nominal bias bound. The weights used in the determination of the projection matrix may be freely selected, however, we will return to this topic later in the paper.

The VPL under the faulted condition is similar except that it adds a faulted bias term

$$VPL_1 = K_{v,md} \sqrt{\sum_{i=1}^N S_{3,i}^2 \sigma_{ff,i}^2} + \sum_{i=1}^N |S_{3,i} b_i| + \max_i |S_{3,i} B_i| \quad (6)$$

Because the occurrence of a fault is unlikely, the value of $K_{v,md}$ can be below 5.33 and we expect it to take a value between 3 and 4 depending on the assigned probability. The term B_i represents the faulted bias and this corresponds to the fault value illustrated at the bottom of Figure 1. The final user VPL is the maximum of the two terms

$$VPL = \max(VPL_0, VPL_1) \quad (7)$$

It is expected that the faulted VPL term will dominate over the fault-free term for most geometries.

NOMINAL ERROR VARIANCE

A critical parameter in the VPL equations described above is the fault-free error variance. This term is fundamentally different from the overbounding error variances used in the current implementation of SBAS. It is intended to only overbound the unfaulted errors and not be inflated to cover any faults. Interestingly, this term was implicitly used in the certification of WAAS for use in guiding aircraft to within 200 feet of the ground. This approach, referred to as a Localizer Precision Vertical – 200 (LPV-200) approach [23] has a requirement that the nominal vertical positioning error be below 4 m 95% and below 10 m 99.99999% [24]. Thus, existing WAAS already has requirements that its unfaulted error terms be bounded by values much smaller than the overbounding integrity variances. In fact, since the system is approved with a Vertical Alert Limit (VAL) of 35 m, but the unfaulted error must be less than 10 m with the same probability, there is an implicit requirement that the unfaulted error distribution be at least 3.5 times smaller than the overbounding error distribution.

This paper proposes to formalize this requirement and make it explicit. This will be difficult because the natural tendency of integrity analyses is to inflate terms to ensure that they are sufficiently large to cover tail events. Instead, this fault-free distribution must be kept very close to actual observed performance, otherwise significant availability will be lost. This variance will need to be empirically determined as it was for the LPV-200 analysis and any outliers scrutinized to determine if they belong to a fault mode instead of a fault-free error distribution. As this is significantly different from previous integrity analyses, we expect that this process will need some time to be developed and accepted. However, we emphasize that this process was already accepted for the

authorization of LPV-200 service, although not explicitly.

In order to determine reasonable values for the fault-free error variances, we turned to the LPV-200 analysis. In this analysis, three years of 1 Hz data was collected and analyzed at 20 locations within WAAS coverage [25]. The Vertical Position Error (VPE) was compared to the VPL (since this was for the operational single-frequency system, the VPL used corresponds to (3)). The plot of VPE versus VPL is reproduced in Figure 2. As can be seen, the actual 95% accuracy numbers are well below the VPL and well below the 4 m requirement. Although the analyses contain more than 1.7 billion data points, there were not sufficient samples to determine the 99.99999% value at each VPL. However, a Gaussian extension of the available probabilities lies below the 10 m requirement, hence the determination that WAAS satisfied the LPV-200 requirements.

We can use these results coupled with independent analyses on the expected accuracies of the various error components to model the fault-free behavior. WAAS continuously evaluates its internal performance and examines the accuracy of its monitors. From previous integrity analyses we know that the accuracy of its UDRE and GIVE monitors is at least three times better than the broadcast confidence. The overbound of the actual observed error is determined for each UDREI and GIVEI index values. These realistic values were placed into our Matlab Availability Analysis Simulation Tool (MAAST) [26], to estimate the expected accuracy for similar conditions to the LPV-200 study. In addition, we used realistic values for the tropospheric error, and the airborne noise and multipath model. For the tropospheric error, we referred to [27] that indicates the nominal standard deviation is 5 cm versus the overbounding value of 12 cm. For the airborne term we referred to a joint paper by Boeing and the FAA [28] that had actual observed curves. We used a simple linear fit to the data in Figures 14 and 16 that showed the actual results varied from about 0.2 m at low elevation to 0.1 m at high elevation.

We then formed a fault-free counterpart to the overbounding variance given by (1)

$$\sigma_{ff,i}^2 = \sigma_{ff,flt,i}^2 + \sigma_{ff,UERE,i}^2 + \sigma_{ff,tropo,i}^2 + \sigma_{ff,air,i}^2 \quad (8)$$

In addition to reducing the variances as described above, the $\delta UDRE$ term was set to unity. This term is used to describe uncertainty associated with satellite clock/ephemeris faults and is described elsewhere [29]. The WAAS safety analysis has observed that it is not needed in the nominal case. The fault-free variance is

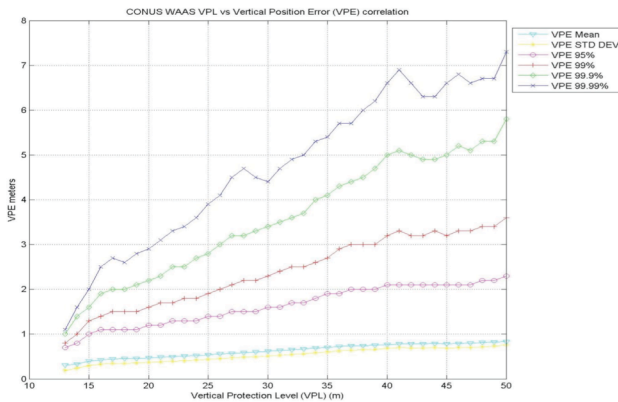


Figure 2. The Vertical Positioning Errors (VPEs) as a function of Vertical Protection Level (VPL) from a three-year study performed on WAAS accuracy [25].

therefore substantially reduced from the integrity overbound version. These terms can be put on the diagonals of a matrix to form the fault-free measurement covariance, \mathbf{Cov}_{ff} . The expected system position covariance matrix can then be determined from this covariance matrix and the projection matrix. The expected 95% accuracy is given by two times the square root of the third diagonal element.

$$95\%Accuracy = 2 \times \sqrt{[\mathbf{S} \cdot \mathbf{Cov}_{ff} \cdot \mathbf{S}^T]_{3,3}} \quad (9)$$

Thus we can compare whether our modeling of the individual range components, combined with the observed geometries, matches the observed position accuracy. Figure 3 presents this comparison where each magenta dot represents a particular instance of a VPL and an expected accuracy value. The black squares and line correspond to the observed 95% value averaged over all stations and times taken from Figure 2. As can be seen, the correspondence is quite remarkable given the differences in the two methods. Thus, we can feel rather confident that we have good starting values for the fault-free variance terms.

As an aside, there is a powerful difference in the determination of the specific expectation of accuracy versus the average accuracy over all conditions. The requirements in the SARPS are actually intended to be specific to the approach conditions, however, the LPV-200 analysis, by necessity, averages over many

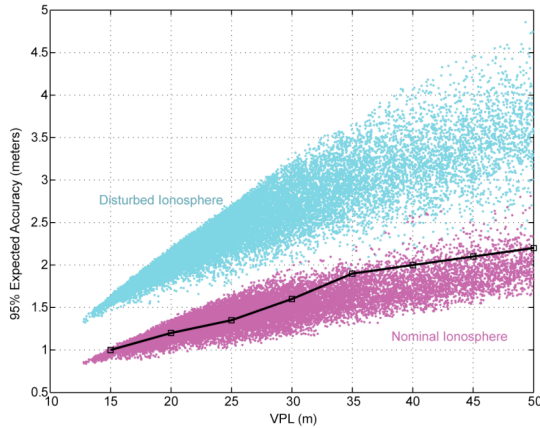


Figure 3. Expected 95% accuracy values as determined by empirical pseudorange error magnitudes and simulated geometries. The magenta points correspond to nominal ionospheric behavior and the light blue points to disturbed ionospheric behavior. The black square and line are the average 95% vertical position errors from Figure 2.

conditions. By matching these two approaches we can perform an analysis of the expected specific accuracy. During the three-year period of the evaluation, all but a few days were under conditions of nominal ionospheric behavior. Because there were so few storm days averaged in, they would have no effect on the overall 95% average. An effort was made to analyze the storm data separately, and an increase in the VPE was seen. However, the WAAS internal evaluations have even better estimates of the observed ionospheric accuracy during disturbed conditions. These storm accuracy values were substituted in for the nominal values to calculate the light blue dots in Figure 3. As can be seen, despite the significant increase in VPE, the accuracy is still expected to be below 4 m in all cases where the VPL is below 35 m. The specific expected accuracy provide by (9) is a much better representation for the instantaneous conditions of the approach. Ideally, this value would be used in place of the overall average.

AVAILABILITY ANALYSIS

Now that we have appropriate estimates for the individual error components, we can construct the dual frequency case. Here we use

$$\sigma_{ff,dual,i}^2 = \sigma_{ff,flt,i}^2 + \sigma_{ff,tropo,i}^2 + (2.6 \times \sigma_{ff,air,i})^2 \quad (10)$$

This can be used as the fault-free variance in (4) and (6).

For comparison we also examined a more conventional adaptation of the single frequency VPL to dual frequency operation. This VPL is much more similar to the single frequency VPL (3). Instead of the single frequency pseudorange overbound given by (1), the dual frequency version uses

$$\sigma_{dual,i}^2 = \sigma_{flt,i}^2 + \sigma_{tropo,i}^2 + (2.6 \times \sigma_{air,i})^2 \quad (11)$$

which is then combined with a nominal bias term to form

$$VPL_{dual,SBAS} = K_{v,PA} \sqrt{\sum_{i=1}^N S_{3,i}^2 \sigma_{dual,i}^2 + \sum_{i=1}^N |S_{3,i} b_i|} \quad (12)$$

This is very similar to the proposed fault-free VPL_0 except that in this case all variances are inflated to the full overbounding value inclusive of possible faults. Thus, this VPL assumes all error sources could be at their maximum values simultaneously.

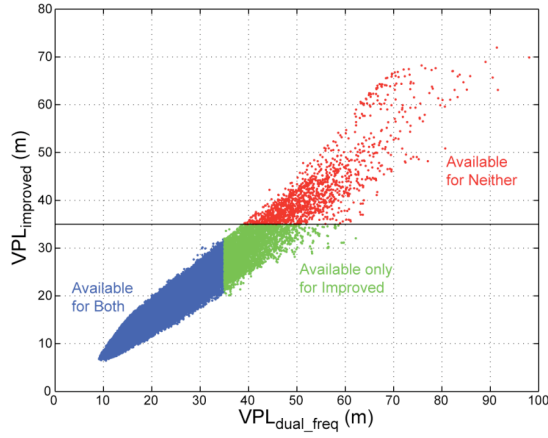


Figure 4. The comparison of the improved VPL proposed in this paper (7) is compared to a more straight-forward implementation described in (12). As can be seen, the improved VPL is about 25% lower than the conventional version

We used MAAST to determine the satellite geometries and expected clock and ephemeris bounds, σ_{flt} , given the WAAS network. MAAST also calculated the two different VPLs on a grid of users around North America. For the conventional VPL (12), σ_{flt} was determined identically to the current WAAS algorithm, the tropospheric term was set to 12 cm per the MOPS [17], the airborne error was as described in the MOPS, and the nominal bias terms were set to a constant .5 m.

For the improved VPL (7), $\sigma_{ff, flt}$ is set to 30% of σ_{UDRE} ($\delta UDRE$ was set to 1 for this term), the tropospheric term

is set to 5 cm, and the airborne term as described in the previous section. The nominal biases were also set to 0.5 m and the faulted bias term was set to 5.33 times σ_{flt} ($\delta UDRE$ takes it full value from MT28 for this term).

Figure 4 compares the two VPL options against each other where the conventional implementation (12) is on the x-axis and the improved version (7) is on the y-axis. As can be seen, the new version proposed here is significantly smaller than the more conventional implementation. On average it is about three-quarters the size and is never larger. Thus, by taking advantage of the expectation of only a single worst-case faulted pseudorange at a time, we can make many more geometries available.

Figures 5 and 6 compare maps of the 99% VPL as a function of location. The colored contours indicate a value that is larger than or equal to 99% of the VPLs that would be obtained at that location during the course of the day. As was evident in Figure 4, Figure 6 shows significant reduction in the VPL versus Figure 5. LPV-200 service is provided even further from the WAAS network concentrated on the North American land mass. Within the primary WAAS region, smaller VPLs are obtained. Thus, there can be significant advantage to explicitly building our existing fault assumptions into the information broadcast to and used by the airborne receiver.

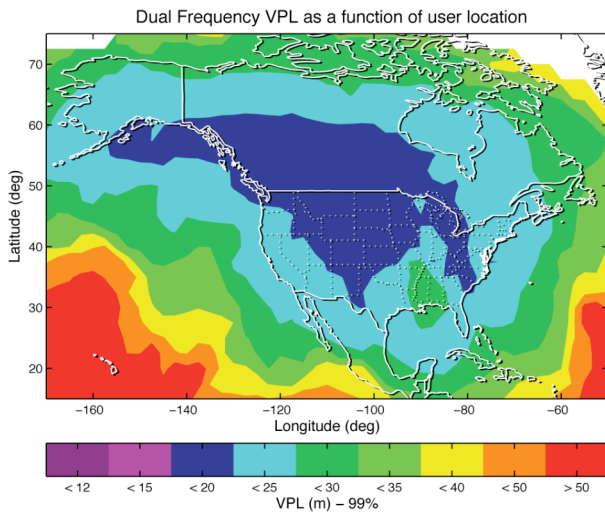


Figure 5. The 99% maximum VPL as a function of user location for the conventional dual frequency VPL described by (12).

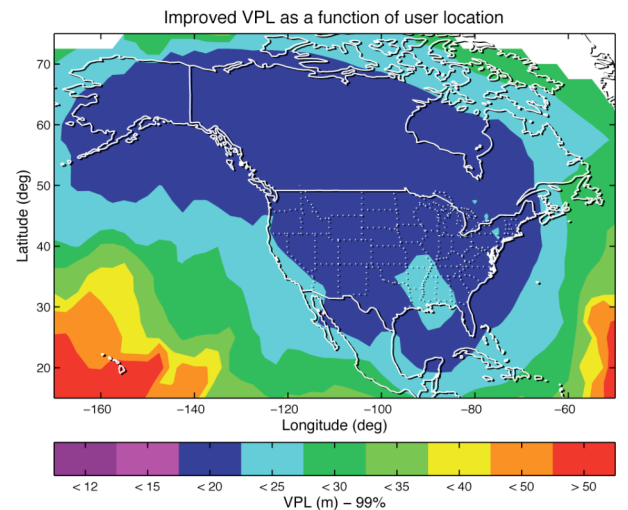


Figure 6. The 99% maximum VPL as a function of user location for the improved dual frequency VPL described by (7).

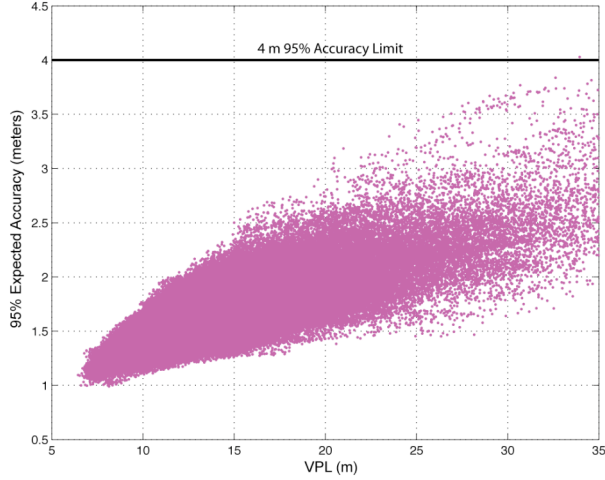


Figure 7. The expected 95% accuracy for each geometry is plotted versus the calculated VPL. Compared to Figures 2 and 3 overall accuracy is worse, but nearly all are below the desired 4 m requirement.

ACCURACY REQUIREMENTS

The previous section demonstrates that significantly more times and locations can be made available. That is, by providing more information on the assumed nominal and faulted modes of the satellites, it is possible to protect against potential 35 m errors in more cases. However, it is not automatic that all other requirements are simultaneously met for these geometries and conditions. In particular, we are concerned about system accuracy, as we know that the dual-frequency iono-free combination may have greater noise than the single frequency iono-corrected pseudorange.

Figure 7 shows the expected accuracy using the same fault-free variances determined by MAAST for the VPL equation and inserting the values into (9) to compute the specific 95% accuracy value for each geometry condition. These are plotted against the corresponding VPL, similarly to what was done for Figure 3. Compared to Figure 3 it is obvious that the accuracy is worse. Of greater concern is that a couple of points actually exceed the desired 4 m limit. Thus, some of the geometries that can have their tail behavior limited to 35 m do not meet our desired performance for accuracy. In an average sense, all geometries do meet the requirement, but by determining the specific accuracy of each situation we can determine that specific cases exist that have worse expectations for accuracy.

It is our recommendation that this test be added to the avionics to disallow these geometries. As there are a relatively small number of instances that fail this test

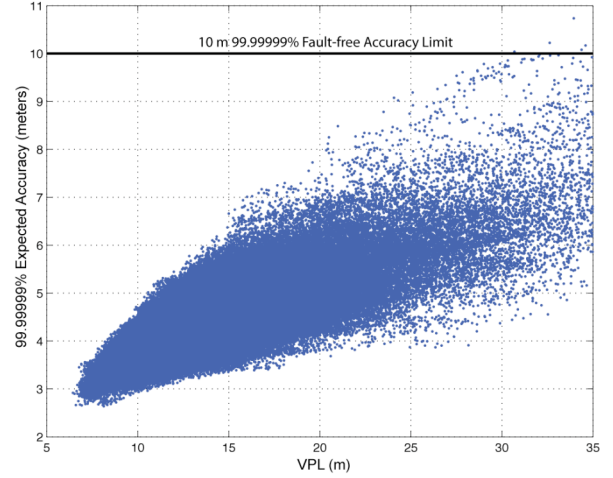


Figure 8. The 99.99999% fault-free accuracy requirement is even more demanding to dual-frequency operation than the 95% accuracy requirement. A small number of geometries do not meet the desired 10 m limit.

compared to the very large number enabled by the change in VPL, there is still a significant increase in availability.

Another accuracy requirement exists and that is that, under fault-free conditions, the 99.99999% accuracy be below 10 m. This accuracy can be estimated by

$$99.99999\% \text{ Accuracy} = 5.33 \times \sqrt{[\mathbf{S} \cdot \mathbf{Cov}_{ff} \cdot \mathbf{S}^T]_{3,3}} \quad (13)$$

This requirement has the same dependence on the geometry and the fault-free variances, but is a more stringent requirement as $10 \text{ m} / 5.33 = 1.88 \text{ m}$, which is less than $4 \text{ m} / 2$.

Figure 8 shows the effect of this requirement. Now a few more geometries should be removed, but still a very small fraction of the much larger number allowed. We recommend that both of these tests be implemented in the avionics, although if this is the correct and final form for these tests, they can be simplified to a single evaluation. In this manner changes that limit the extreme values of the error distribution are also evaluated for their impact on the core of the distribution.

FUTURE OPTIMIZATIONS

The L1-only VPL equation has no bias terms. Therefore, the optimal weights for minimizing the VPL equation are the ones specified in the MOPS. However, the VPL proposed here in (7) includes both nominal and faulted bias terms. The optimal weight is thus unlikely to be the

inverse of the covariance matrix. From (6) it is intuitive that the weight for the dominant satellite can be increased to reduce the value of $S_{3,i}$. The weights can be optimized such that this term is equal across all satellites. However, this weight selection may be very different from the set of weights that optimize accuracy. This latter set of weights would be the inverse of the fault-free covariance matrix.

Given that we have these competing goals, it is important to track accuracy and integrity specifically. For this paper we have chosen weights based upon the conventional inverse of the overbounding variances. We anticipate that optimizing the weights in order to minimize the maximum fault bias contribution will lead to an additional significant reduction in VPL as has been found for ARAIM [13]. However, have not yet confirmed this nor tested the resulting effect on accuracy.

CONCLUSIONS

This paper proposes a specific form for the dual frequency SBAS protection level equations. These equations exploit the iono-free combination of L1 and L5 GPS signals to eliminate the largest source of uncertainty affecting the current single-frequency SBAS equations. Further, the removal of the ionospheric influence also eliminates the only significant source of large range errors that are likely to affect more than one range measurement at a time. Therefore, we propose that the new equation treat all satellites but one, as operating under nominal error distributions, with the one satellite possibly being affected by the worst-case undetected error. We also include nominal error bias terms to account for small unobservable range biases and for non-Gaussian behavior of the underlying error distribution.

We demonstrate that the existing SBAS implementation already requires that WAAS maintain small nominal error distributions in order to support the LPV-200 operation and that the approach advocated here merely formalizes this dependence. We further show, that by taking this approach, we significantly reduce the VPL. This reduction provides improved availability and continuity of service against the most stringent supported operation, LPV-200. The approach also provides a real-time estimate of the expected accuracy. The accuracy should also be evaluated in the aircraft to ensure that future system changes continue to meet operational requirements.

The proposed VPL equation is also better matched to the WAAS hazard analysis. This will make subsequent

analyses of system safety easier as there is better correspondence between what is required for certification and the information provided to the user. Finally, we expect to gain even smaller VPLs when we optimize the weights used in the position estimate.

ACKNOWLEDGMENTS

The authors would like to gratefully acknowledge discussions that have taken place with various member of the WAAS Integrity Performance Panel. The FAA Satellite Product Team, under Cooperative Agreement 2008-G-007, supported the work for this paper.

REFERENCES

- [1] McDonald, K. D. and Hegarty, C., "Post-Modernization GPS Performance Capabilities," Proceedings of ION annual Meeting, San Diego, CA, 2000.
- [2] Van Dierendonck, A. J., Hegarty, C., Scales, W., and Ericson, S., "Signal Specification for the Future GPS Civil Signal at L5," Proceedings of ION annual Meeting, San Diego, CA, 2000.
- [3] Hegarty, C. J. and Chatre E., "Evolution of the Global Navigation Satellite System (GNSS)," in Proceedings of the IEEE Vol. 96, Issue 12, Dec. 2008.
- [4] Walter, T. and Enge, P., "The Wide-Area Augmentation System," Chapter 4.1 in EGNOS The European Geostationary Overlay System, ESA publication SP-1303, December, 2006.
- [5] Lawrence, D., "Wide Area Augmentation System (WAAS) Program Status," Proceedings of the 21st International Technical Meeting of the Satellite Division of The Institute of Navigation (ION GNSS 2008), Savannah, GA, September 2008, pp. 1009-1031.
- [6] Rife, J., Pullen, S., Pervan, B., and Enge, P. "Paired Overbounding and Application to GPS Augmentation" Proceedings of the IEEE Position Location and Navigation Symposium, Monterey, CA, April 2004.
- [7] Walter, T., Rife, J., and Blanch, J., "Treatment of Biased Error Distributions in SBAS," in proceedings of GNSS 2004, Sydney, Australia, December 2004.

- [8] Walter, T., Blanch, J., and Enge, P., "L5 Satellite Based Augmentation Systems Protection Level Equations," in Proceedings of the International GNSS conference, Sydney, Australia, December, 2007.
- [9] Walter, T., Blanch, J., Enge, P., "Evaluation of Signal in Space Error Bounds to Support Aviation Integrity," Proceedings of the 22nd International Technical Meeting of The Satellite Division of the Institute of Navigation (ION GNSS 2009), Savannah, GA, September 2009, pp. 1317-1329.
- [10] Rodriguez, C., "Ground Based Augmentation System (GBAS) Local Area Augmentation System (LAAS) Program Status," Proceedings of the 21st International Technical Meeting of the Satellite Division of The Institute of Navigation (ION GNSS 2008), Savannah, GA, September 2008, pp. 994-1008.
- [11] Walter, T., Blanch, J., Enge, P., Pervan, B., and Gratton, L., "Future Architectures to Provide Aviation Integrity," in proceedings of ION NTM, San Diego, CA, January, 2008.
- [12] Walter, T., Enge, P., Blanch, J., and Pervan, B., "Worldwide Vertical Guidance of Aircraft Based on Modernized GPS and New Integrity Augmentations," Proceedings of the IEEE Vol. 96, Issue 12, Dec. 2008.
- [13] Blanch, J., Walter, T., and Enge, P., "RAIM with Optimal Integrity and Continuity Allocations Under Multiple Fault Conditions," in IEEE Transactions on Aerospace and Electronic Systems, Vol. 46, No. 3, July 2010, pp. 1235-1247.
- [14] Oehler, V., Luongo, F., Boyero, J., Stalford, R., Trautenberg, H. L., Hahn, J., Amarillo, F., Crisci, M., Schlarmann, B., Flamand, J.F., "The Galileo Integrity Concept," Proceedings of the 17th International Technical Meeting of the Satellite Division of The Institute of Navigation (ION GNSS 2004), Long Beach, CA, September 2004, pp. 604-615.
- [15] Lee, Y. C., Fernow, J. P., "Analysis of GPS RAIM Continuity and Availability for Oceanic RNP Operations," Proceedings of the 49th Annual Meeting of The Institute of Navigation, Cambridge, MA, June 1993, pp. 287-304.
- [16] Walter, T., Enge, P., and Hansen, A., "A Proposed Integrity Equation for WAAS MOPS," in proceedings of ION GPS-97, pp. 475-484, Kansas City, MO, September 1997.
- [17] RTCA, "Minimum Operational Performance Standards for Global Positioning System/Wide Area Augmentation System Airborne Equipment," RTCA publication DO-229D, 2006.
- [18] Schempp, T. R., Rubin, A. L., "An application of Gaussian Overbounding for the WAAS fault free error analysis," Proceedings of the 15th International Technical Meeting of the Satellite Division of The Institute of Navigation (ION GPS 2002), Portland, OR, September 2002, pp. 766-772.
- [19] Heng, L., Gao, G.X., Walter, T., and Enge P., "GPS Signal-in-Space Anomalies in the Last Decade," Proceedings of the International Technical Meeting of the Satellite Division of The Institute of Navigation (ION GNSS 2010), Portland, OR, September 2010
- [20] Phelts, R.E., Walter, T., Enge, P., "Characterizing Nominal Analog Signal Deformation on GNSS Signals," Proceedings of the 22nd International Technical Meeting of The Satellite Division of the Institute of Navigation (ION GNSS 2009), Savannah, GA, September 2009, pp. 1343-1350.
- [21] DeCleene, B., "Defining Pseudorange Integrity - Overbounding," Proceedings of the 13th International Technical Meeting of the Satellite Division of The Institute of Navigation (ION GPS 2000), Salt Lake City, UT, September 2000, pp. 1916-1924.
- [22] "Minimum Operational Performance Standards for GPS Local Area Augmentation System Airborne Equipment," Washington, D.C. RTCA SC-159 WG-4A, DO-253A, November 28, 2001.
- [23] Cabler, H., DeCleene, B., "LPV: New, Improved WAAS Instrument Approach," Proceedings of the 15th International Technical Meeting of the Satellite Division of The Institute of Navigation (ION GPS 2002), Portland, OR, September 2002, pp. 1013-1021.
- [24] International Civil Aviation Organization (ICAO) International Standards and Recommended Practices (SARPs), Aeronautical Telecommunications Annex 10, Volume I, Radio Navigation Aids, 2010.
- [25] Wanner, B., and Nelthropp, D., "Wide Area Augmentation System, LPV200 Vertical Accuracy Assessment," Presentation to ICAO NSP, October, 2006.
- [26] Jan, S.S., Chan, W., Walter, T., Enge, P., "Matlab Simulation Toolset for SBAS Availability Analysis," Proceedings of the 14th International Technical Meeting

of the Satellite Division of The Institute of Navigation (ION GPS 2001), Salt Lake City, UT, September 2001, pp. 2366-2375.

[27] Collins, J. P., Langley, R. B., “The residual tropospheric propagation delay: How bad can it get?,” Proceedings of the 11th International Technical Meeting of the Satellite Division of The Institute of Navigation (ION GPS 1998), Nashville, TN, September 1998, pp. 729-738.

[28] Murphy, T., Harris, M., Booth, J., Geren, P., Pankaskie, T., Clark, B., Burns, J., Urda, T., “Results from the Program for the Investigation of Airborne Multipath Errors,” Proceedings of the 2005 National Technical Meeting of The Institute of Navigation, San Diego, CA, January 2005, pp. 153-169.

[29] Walter, T., Hansen, A., Enge, P., “Message Type 28,” Proceedings of the 2001 National Technical Meeting of The Institute of Navigation, Long Beach, CA, January 2001, pp. 522-532.

APPENDIX: HPL

The corresponding Horizontal Protection Level (HPL) can simply be found by determining bounds in the East and North directions and RSSing them together. Thus, one possible form of the unfaulted HPL would be

$$HPL_0^2 = \left(K_{H,PA} \sqrt{\sum_{i=1}^N S_{1,i}^2 \sigma_{ff,i}^2} + \sum_{i=1}^N |S_{1,i} b_i| \right)^2 + \left(K_{H,PA} \sqrt{\sum_{i=1}^N S_{2,i}^2 \sigma_{ff,i}^2} + \sum_{i=1}^N |S_{2,i} b_i| \right)^2 \quad (14)$$

where $K_{H,PA}$ corresponds to the Gaussian tail and is expected to be 5.73, $S_{1,i}$ and $S_{2,i}$ are the first and second elements of the i^{th} row of the projection matrix. They represent the effect on the horizontal position error due to an error on the ranging measurement to the i^{th} satellite. The remaining terms are as described below (4).

The HPL under the faulted condition is given by

$$HPL_j^2 = \left(K_{H,md} \sqrt{\sum_{i=1}^N S_{1,i}^2 \sigma_{ff,i}^2} + \sum_{i=1}^N |S_{1,i} b_i| + S_{1,j} B_j \right)^2 + \left(K_{H,md} \sqrt{\sum_{i=1}^N S_{2,i}^2 \sigma_{ff,i}^2} + \sum_{i=1}^N |S_{2,i} b_i| + S_{2,j} B_j \right)^2 \quad (15)$$

As with the VPL, because the occurrence of a fault is unlikely, the value of $K_{H,md}$ can be below 5.73 and we expect it to take a value between 4 and 5 depending on the assigned probability. The final user HPL is the maximum of the terms

$$HPL = \max_j (HPL_0, HPL_j) \quad (16)$$

There may be more optimal formulations of the HPL, but because GPS is generally better performing in the horizontal direction and the aviation requirements are less demanding, it is not critical to optimize the HPL.

The horizontal accuracy should also be evaluated in the aircraft and it is obtained through

$$2.45 \times \sqrt{[\mathbf{S} \cdot \mathbf{Cov}_{ff} \cdot \mathbf{S}^T]_{1,1}} + [\mathbf{S} \cdot \mathbf{Cov}_{ff} \cdot \mathbf{S}^T]_{2,2} \quad (17)$$

for the 95% horizontal accuracy and

$$5.68 \times \sqrt{[\mathbf{S} \cdot \mathbf{Cov}_{ff} \cdot \mathbf{S}^T]_{1,1}} + [\mathbf{S} \cdot \mathbf{Cov}_{ff} \cdot \mathbf{S}^T]_{2,2} \quad (18)$$

for the 99.999999% fault-free horizontal accuracy.